

See discussions, stats, and author profiles for this publication at: <https://www.researchgate.net/publication/331287853>

# Autogenous mineral textures in micropores and microcracks, Roman architectural concrete, Markets of Trajan, Rome

Conference Paper · May 2017

CITATION

1

READS

389

4 authors:



**Marie Jackson**

University of Utah

72 PUBLICATIONS 2,394 CITATIONS

SEE PROFILE



**Yi Zhang**

National University of Singapore

6 PUBLICATIONS 87 CITATIONS

SEE PROFILE



**Heng Chen**

University of Jinan (China)

55 PUBLICATIONS 1,150 CITATIONS

SEE PROFILE



**Juhyuk Moon**

Seoul National University

161 PUBLICATIONS 5,159 CITATIONS

SEE PROFILE

# Autogenous mineral textures in micropores and microcracks, Roman architectural concrete, Markets of Trajan, Rome

JACKSON Marie<sup>1,a</sup>, ZHANG Yi<sup>2,b</sup>, CHEN Heng<sup>3,c</sup>, MOON Juhuk<sup>2,d\*</sup>

<sup>1</sup>Department of Geology and Geophysics, University of Utah, Salt Lake City, UT, 84112, USA

<sup>2</sup>Department of Civil and Environmental Engineering, National University of Singapore, 117576, Singapore

<sup>3</sup>School of Materials Science and Engineering, Southeast University, Nanjing, 211189, Peoples Republic of China

<sup>a</sup>m.d.jackson@utah.edu, <sup>b</sup>e0022713@u.nus.edu.sg, <sup>c</sup>hengchen08@gmail.com, <sup>d</sup>ceemjh@nus.edu.sg

\*corresponding author

14<sup>th</sup> International Conference on Durability of Building Materials and Components  
Gent, Belgium, 29-31 May 2017

**Keywords:** Roman architectural concrete, Computed tomography, Durability, Microcracks, Strätlingite

## Abstract.

Concrete wall structures of the Markets of Trajan, constructed ~110 CE in Rome, have remained resistant to fracture and chemical decay for nearly 2000 years. New investigations with X-ray microtomography (XMT) indicate, however, that the volcanic ash-hydrated lime mortar that binds the conglomeratic concrete is a highly porous material. This contrasts with a low porosity requirement for high durability in modern cement-based concrete. New investigations with synchrotron-based X-ray microdiffraction (XRMD) indicate, by contrast, that the poorly-crystalline, calcium-aluminium-silicate-hydrate (C-A-S-H) binder of the ancient mortar is reinforced with strätlingite, a resilient phyllosilicate mineral with 12.5 Å interlayer d-spacing. To gain insights into Roman imperial era concrete technologies that can provide guiding principles for extending the longevity of modern concrete compositions with volcanic rock pozzolans, we use XRMD and XMT to explore porosity associated with microscale mortar components – the cementing matrix, spherical pores, and segmented *en echelon* microcracks. Strätlingite mineral textures traverse micropores 500 µm in diameter, apparently blocking propagation of microcracks at the sub-millimetre scale. In the cementing matrix, linkages of microcrack segments contain dense arrays of shorter microcracks, ≤100 µm in length. The high surface roughness of these bridging microstructures indicate that large fracture energy is required for crack propagation through the cementing matrix. The high toughness may result, in part, from obstacles presented by relicts of microscoria and pervasive strätlingite plates. Calcite crystals frequently fill the porosity created by the microcrack surfaces, possibly leading to further toughness. Although Roman builders may not have been aware of these autogenous processes, their standardized selection of scoriaceous ash from the highly potassic, mid-Pleistocene Pozzolane Rosse pyroclastic flow apparently generated alkali-activated strätlingite crystallization and long-term calcite crystallization that has ensured the resilience of the porous concrete for nearly two millennia.

## Introduction

The Markets of Trajan are a vast complex of buildings, constructed of brick-faced conglomeratic concrete about 98–117 CE on the south side of the Quirinale Hill overlooking the Forum of Trajan in Rome [1]. The buildings remain in use today as the Museo dei Fori Imperiali [2]. They have resisted fracture and decay associated with frequent moderate magnitude earthquakes ( $IS < 8$  MCS) for nearly 2000 years [3, 4]. The architectural focus of the complex is a Great Hall, which has a 32 m tall by 8 m

wide vaulted ceiling supported by one-meter thick walls of brick-faced concrete [5]. Decimeter-sized volcanic tuff and brick aggregate in the internal conglomeratic wall core is bound by a highly durable volcanic ash-hydrated mortar [6] (Fig. 1). The fundamental binding component of the mortar is complex cementing matrix, composed of poorly-crystalline calcium-aluminium-silicate-hydrate (C-A-S-H) binder containing alkali cations, the relicts of partially reacted scoriaceous ash particles, and platy strätlingite, a resilient calcium-aluminium-silicate phyllosilicate with 12.5 Å [0001] interlayer spacing [6, 7].

A fracture mechanics study of a reproduction of the Markets of Trajan wall mortar using high calcium quicklime and scoriaceous ash from the highly-potassic, mid-Pleistocene Pozzolane Rosse pyroclastic flow, erupted from nearby Alban Hills volcano [8], demonstrates that much of the resilience of the concrete results from the growth of platy strätlingite crystals [9, 10]. The crystals begin to grow before 90 days' hydration, after portlandite is consumed through pozzolanic reaction. Fracture testing of the young mortar using an innovative three-point-bending test indicates that strength increases as C-A-S-H begins to coalesce between 28 and 90 days hydration, and toughness increases from 90 to 180 days hydration as fine (<1–3 µm) strätlingite fibres and plates present obstacles to microcrack propagation in the cementitious matrix and the interfacial zones of scoria. The 180-day mortar produces values for Young's modulus and uniaxial tensile strength about 1/10 of modern structural concrete, but the fracture energy ( $G_F$ , joules per square meter), the amount of mechanical work required to propagate a macrocrack to create one square unit of new surface area [11], is close to one-half [10].

The Markets of Trajan wall mortar contains abundant strätlingite [6, 10], but little is known about how these crystals are distributed through the 1900-year-old mortar fabric and how they might specifically mitigate the propagation of microcracks at sub-millimetre length scales. The crystals commonly occur as bundles of intergrown plates up to 100 µm in length (Fig. 1b, c, d). These textures suggest long-term and, perhaps, ongoing crystallization processes that are important to the resilience of the concrete, since the mortar is a highly porous material. For example, Pozzolane Rosse scoriae, which act as both fine sand-sized pozzolan and as sand- to gravel-sized aggregate, contain large irregularly-shaped vesicles; the cementing matrix contains pores up to 1–2 mm in diameter; and relict microcracks, produced when the concrete fractured in response to static and seismic loading, may increase porosity over the long service life of the monument.

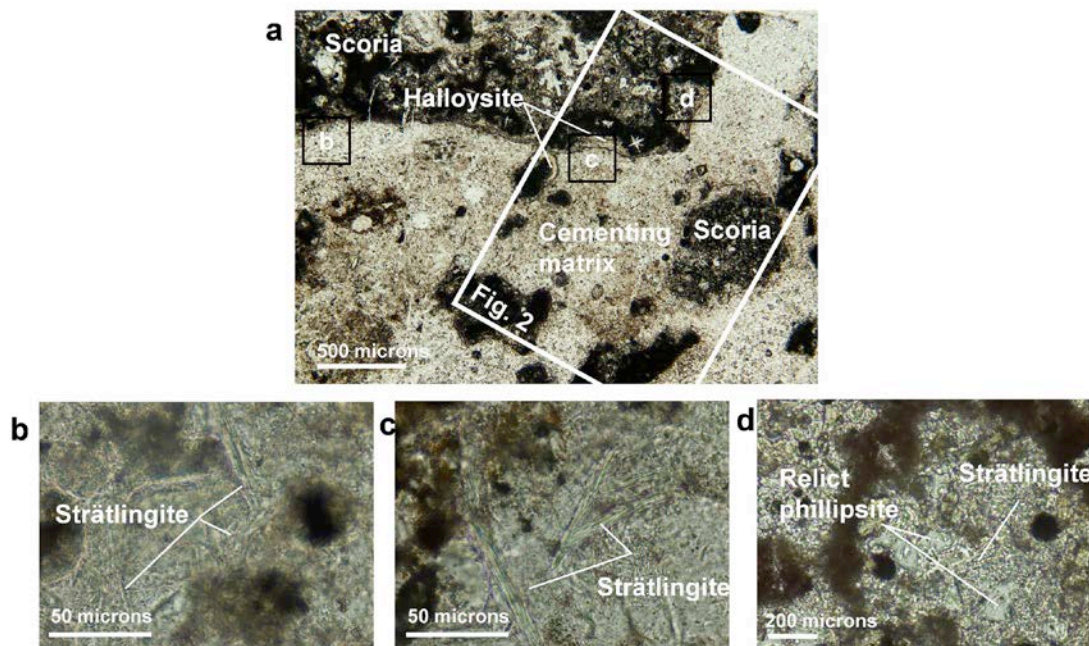


Fig. 1. Petrographic images, plane polarized light, of mortar from a drill core of Markets of Trajan concrete. a) Overview of the area investigated with synchrotron-based XRMD (Fig. 2). b, c, d) Strätlingite crystallization in the cementitious matrix and a scoria vesicle.

Here, synchrotron-based X-ray microdiffraction (XRMD) investigations describe the distribution of strätlingite crystals in diverse components of the mortar fabric: the cementing matrix, interfacial transition zones of scoria with the cementing matrix, and scoria vesicles with relicts of geologic textures, mainly clay mineral and zeolite. X-ray microtomography (XMT) investigations describe two predominant components of the porous mortar fabric: spherical pores in the cementing matrix and relict microcracks. The results of these investigations provide new insights into autogenous crystallization of post-pozzolan mineral textures, mainly strätlingite and calcite, in micropores and microcracks. These cementitious textures record potentially self-healing processes that have enhanced the durability and resilience of the porous mortar over nearly two millennia.

## Materials and Methods

The very well-consolidated conglomeratic concrete comes from a 4-cm-diameter core (core 11-MT-C1) drilled into the deep foundational walls of the southern, lower levels of the Markets of Trajan near the via Biberatica and from a 20-cm-diameter core, drilled into the eastern supporting wall of the Great Hall (core GRAULA-20A). Both mortars have the same composition [10]. The cores were wrapped in plastic to minimize exposure to the atmosphere and carbonation of cementitious phases. Preparation of thin sections utilized hydrophobic methods.

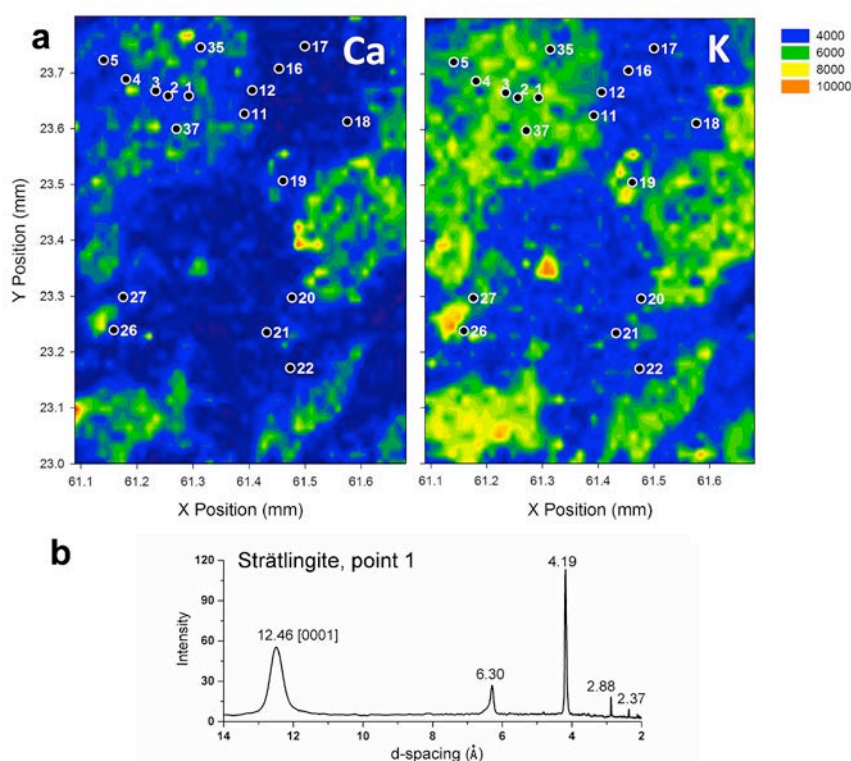


Fig. 2. Sites of XRMD analyses in the mortar fabric showing strätlingite diffraction patterns (Fig. 1a). a) X-ray Fluorescence (XRF) maps show qualitative concentrations of calcium and potassium, ranging from red (highest) to blue (lowest), and points with strätlingite d-spacing. b) A typical strätlingite diffraction pattern, located at point 1.

**X-ray Microdiffraction.** Crystalline cementitious phases were identified in the Markets of Trajan wall mortar using XRMD at beamline 12.3.2 of the Advanced Light Source at the Lawrence Berkeley National Laboratory, Berkeley, USA. A thin slice of mortar was removed from a polished thin section of Markets of Trajan wall concrete, which had been previously characterized with petrographic analyses (Fig. 1). The beamline uses a superconducting bending magnet as a source to deliver an X-ray spectrum ranging from 5 to 22 keV. In this experiment, a monochromatic X-ray beam of 10 keV was focused to 2 (v) × 24 (h) μm diameter, and the sample was placed in transmission mode into



the beam, with the detector  $2\theta$  at  $39^\circ$ . A Pilatus1M area detector was placed at 150 mm to record Debye rings diffracted by the crystalline phases. Debye diffraction rings were then radially integrated into intensity versus d-spacing plots over an arch segment of  $76^\circ$  for  $2\theta$   $3^\circ$ – $45^\circ$ . X-ray microfluorescence analyses record the qualitative contents of calcium, potassium, iron, titanium over the area of interest, and assist with correlating the sites of analyses with microscopic images (Fig. 2, counts increase from red to blue).

**X-ray Microtomography.** XMT investigations probe the internal structure of a sample using a non-destructive X-ray beam, so that delicate, fine-scale components of a mortar are preserved and can be described in detail. Here, XMT is used to construct a series of two-dimensional (2D) tomographic slices and three-dimensional (3D) volumetric rendering images of a small hand sample of mortar from the eastern supporting wall of the Great Hall of the Markets of Trajan. The mortar has the same composition as that of the XRMD analyses (Figs. 1, 2). The irregularly shaped mortar specimen (Fig. 3) was analysed using a commercially available Bruker MicroCT (Bruker, Germany). Using an experimental setting of 50 kV and 150 amps, 1000 low resolution 2D tomographic images ( $8.5\ \mu\text{m}/\text{pixel}$ ) were obtained, with a size of 1012 pixels by 1024 pixels each. The identification of discrete pores (shown in white, Fig. 3a, b, d, e) was possible, through selecting threshold values to distinguish these from the cementing matrix (light grey) and the scoriaceous volcanic ash aggregate (dark grey), which contains about 10–11 weight%  $\text{Fe}_2\text{O}_3$  and 4–5 weight% MgO [8] (Fig. 4). Note that the 2D slice images were inverted for better readability. This means that the original 2D slice images had pores as black and the iron- and magnesium-rich aggregates as bright to dark grey. A 3D construction was then made of the bulk mortar specimen from these images (Fig. 3c, f). Next, with a different experimental setting, 80 kV and 100 amps, higher resolution images ( $2.0\ \mu\text{m}/\text{pixel}$ ) were obtained from the cylindrical shape shown in Fig. 3c. These 2D slice images are 976 pixels by 1003 pixels each (Fig. 3d, e). The locations of the images in the cylindrical shape (Fig. 3c, f) were selected to illustrate certain instructive microstructures pertaining to relict porosity associated with spherical pores and segmented microcracks (Figs. 5, 6).

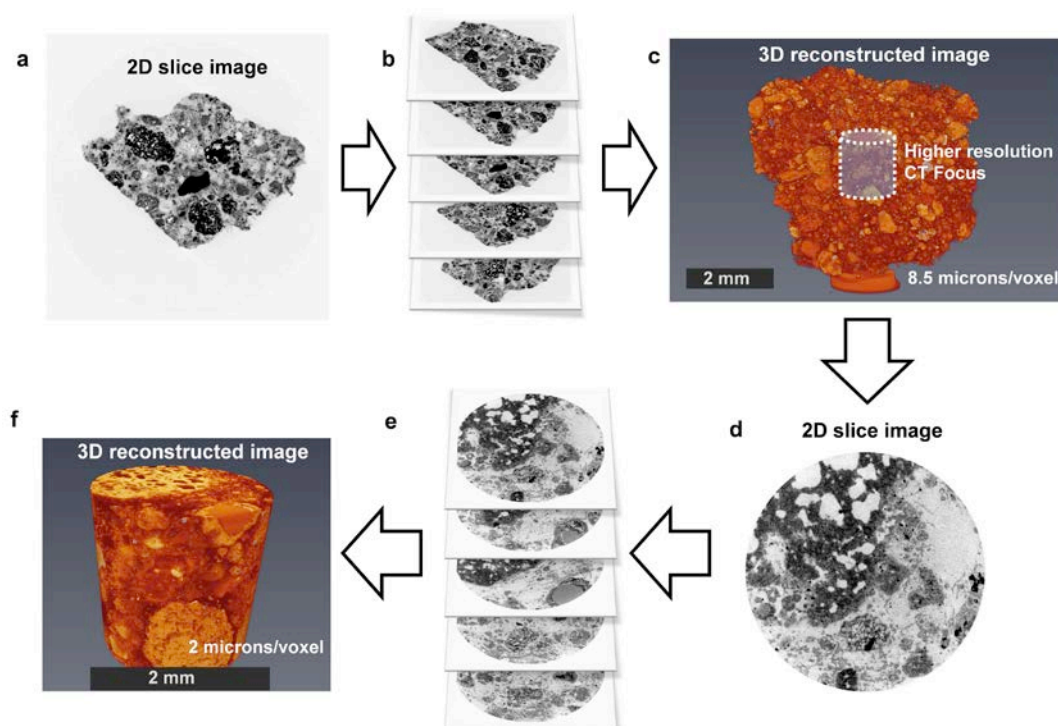


Fig. 3. The two-stage X-ray microtomography (XMT) analysis. a, b, c) A first set of investigations was obtained from a small specimen of the mortar, with a resolution of  $8.5\ \mu\text{m}/\text{pixel}$ . d, e, f) A second set of investigations was obtained from a cylindrical shape in the centre of the same specimen, with a higher resolution of  $2.0\ \mu\text{m}/\text{pixel}$ .

AVIZO Fire image processing software (VSG, France) was used for volumetric rendering and image segmentation. Different threshold values, scaled from 0 to 256, were applied to quantitatively differentiate discrete phases in the 3D constructed image (Fig. 4). Through visual inspection, values of 19-60, 60-108, 109-178, and 179-255, were selected to segment, respectively, pores and scoria vesicles, the cementing matrix, the scoriaceous volcanic ash aggregate, and other volcanic ash components, mainly crystals of leucite. Relict microcracks appear as light grey, suggesting that there is not a straightforward void space between the crack walls.

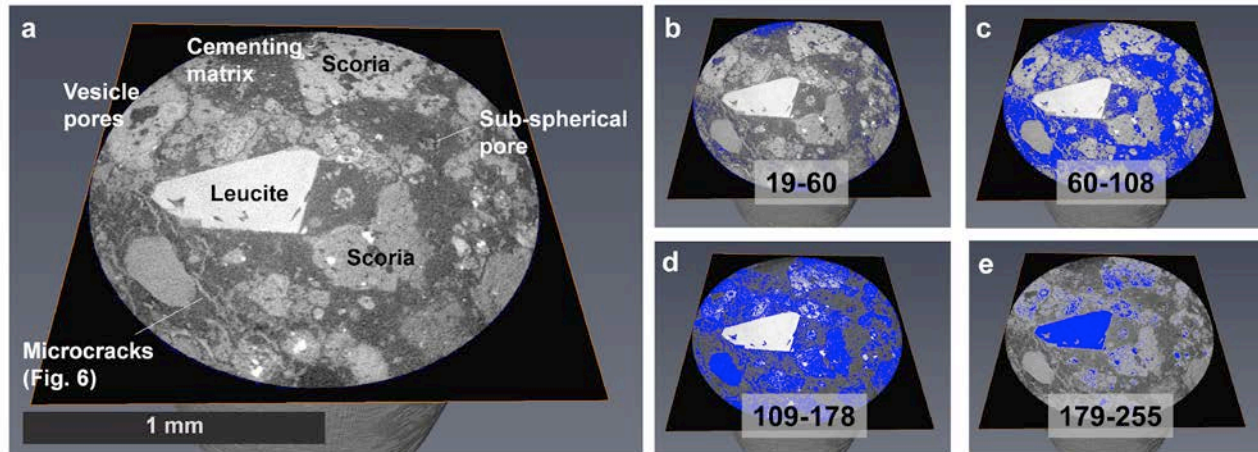


Fig. 4. Images showing the selection of thresholding values to segment phases (shown in blue) in the 3D high resolution volumetric images (Fig. 3d–e). a) Components of the mortar fabric. b, c, d, e) Selected values of 19-60, 60-108, 109-178, and 179-255 indicate, respectively, empty pores, the cementing matrix, the scoriaceous volcanic ash aggregate, and other volcanic ash components, mainly crystals of leucite, a potassic framework silicate. Microcracks fall in the 109-178 range.

### Cementing Components

The macro-scale fabric of the wall mortar shows the characteristic features of the highest quality Trajanic era concretes. Large dark grey (Munsell Color N2) to dark dusky red (10R 2/2 to 5R 3/4) scoriae, up to 2–3 cm in diameter, from the Pozzolane Rosse pyroclastic flow form the coarse aggregate of the mortar. These have authigenic clay mineral and zeolite surface coatings (Fig. 1), produced by interaction of surface and ground water with the highly-reactive alkali-rich volcanic glass and crystals in the pyroclastic flow deposit [8]. The halloysite clay mineral, zeolite, principally phillipsite and chabazite, and volcanic glass have pozzolanic properties, and are used as pozzolans in modern Portland cement concretes [12]. A complex cementing matrix, nearly translucent in plane polarized light (Fig. 1), is composed of poorly-crystalline C-A-S-H binder with  $\text{Ca}/(\text{Si}+\text{Al}) = 0.45\text{--}0.75$  [10], interspersed with partially-dissolved, fine sand-sized particles of Pozzolane Rosse volcanic ash. Networks and bundles of 50–100  $\mu\text{m}$  strätlingite crystals, identified through optical techniques, have grown through the C-A-S-H binder (Fig. 1b). The crystals are also associated with relict halloysite clay mineral coatings in the interfacial transition zone of scoria with the cementing matrix (Fig. 1c), and with coatings of phillipsite, a potassic zeolite (Fig. 1d) on the internal surfaces of scoria vesicles.

Qualitative X-ray micro-fluorescence maps (Fig. 2) show elevated concentrations of calcium, mainly in scoria vesicles, and potassium, mainly concentrated in the relict glassy groundmass and leucite crystals of Pozzolane Rosse scoriae. On these maps, the numbered points indicate locations of X-ray microdiffraction analyses, taken from a  $2\text{--}3\ \mu\text{m}^2$  spot size, which show strätlingite d-spacings. Taken together, the analyses indicate that strätlingite occurs within the C-A-S-H of the cementing matrix (points 16, 17), the dissolved rims of fine sand-sized scoriae (points 18, 19, 21, 22), the interfacial zones of sand- to gravel-sized scoriae (points 11, 12, 20, 26, 27), and the internal vesicular structure of scoriae (points 1–5, 35, 37). The wide range of crystallization environments suggests multiple chemical mechanisms and episodes of strätlingite formation. These are likely related to

macroscale and microscale variations in the permeability, porosity and reactivity of the host material components, and are the subject of ongoing research.

### Relict Pores, Cementing Matrix

The mortar of Markets of Trajan wall concrete has a high cumulative porosity, produced by irregularly-shaped vesicles in scoria clasts, up to 1–2 mm, and pores in the cementing matrix, up to 1–2 mm in diameter. Water absorption measurements of the wall mortar range from 12–26 weight% [6]. These high values suggest a large relative volume of empty space that should, in principle, result in lower resistance to fracture. They also indicate that when water saturated, as occurred frequently during Tiber River floods and ground water penetration into the monument [13], the mortar and volcanic tuff aggregate [14] hold a great deal of moisture. Interaction of this interstitial water with the reactive components of Pozzolane Rosse volcanic ash aggregate – highly potassic volcanic glass, leucite crystals, and authigenic clay mineral and phillipsite surface coatings – at ambient temperatures could potentially produce post-pozzolanic cementitious processes. Such authigenic cementitious processes have produced strätlingite crystals in alkali-rich, phonolitic lava near Rome [15].

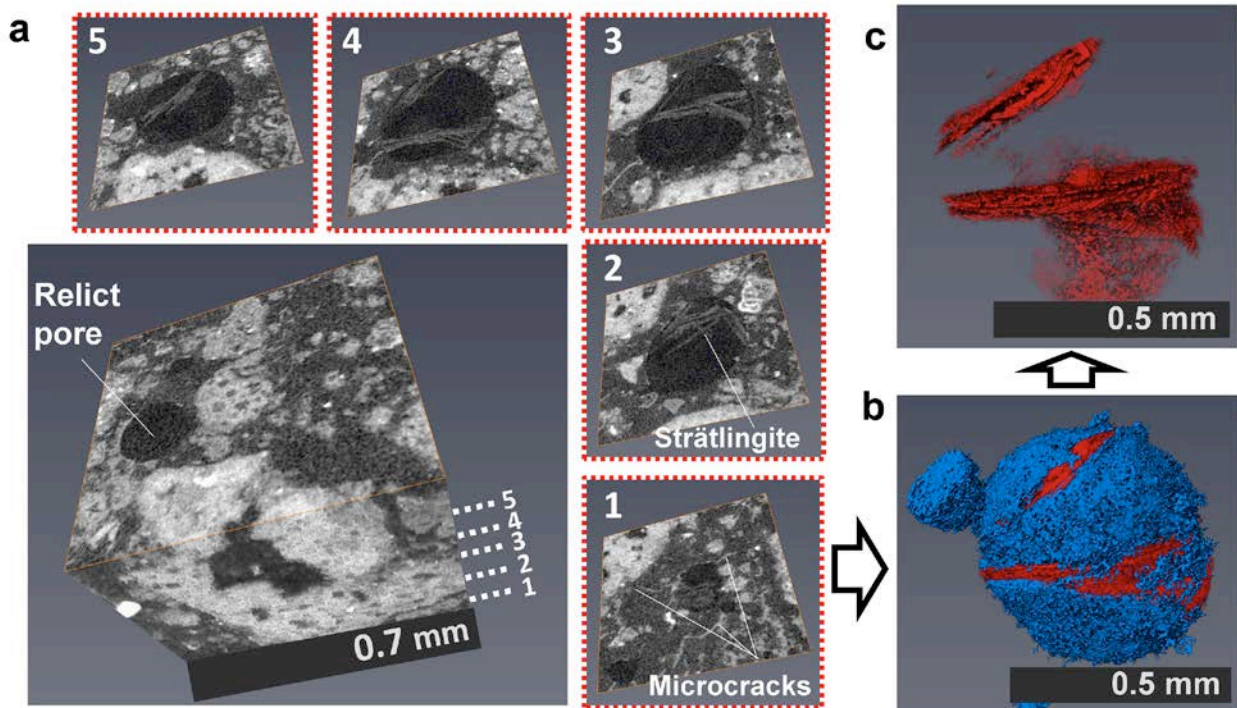


Fig. 5. Reconstruction of a typical sub-spherical pore in the cementing matrix. a) 3D reconstruction and 2D image slices of the 500 µm diameter pore and associated microcrack terminations. b) 3D reconstruction of the pore (blue), which is partially filled by platy strätlingite (red) intergrowths, with long axes ranging from 10–200 µm.

Strätlingite crystals commonly span vesicle cavities in scoriae. They also traverse nearly all the sub-spherical pores in the cementing matrix. For example, Fig. 5a shows strätlingite crystals in a sub-spherical pore, 500 µm in diameter. The 3D reconstruction shows the cementing matrix (blue) that form the walls of the pore (Fig. 5b) and the complex intergrowths of strätlingite (red) ranging from 10–200 µm in the pore (Fig. 5c). These are not simply acicular, fibre-like crystals as might be inferred from the 2D tomographic images. Instead, they are arrays of crystals that grew in diverse orientations. In addition, there are three fine microcracks that terminate at the pore wall (Fig. 5a (1)). These apparently did not propagate across the pore to form longer crack structures. It may be that the



microcracks post-date strätlingite crystallization, and that the crystal plates formed three-dimensional obstacles to further crack growth.

### Relict Microcracks, Cementing Matrix

Fracture testing experiments of a reproduction of the Markets of Trajan wall mortar produced segmented microcracks at 90 and 180 days' hydration [10]. Offsets of the segments commonly occurred near sand- and gravel-sized scoriae and leucite crystals, which obstructed crack growth at the millimetre scale. Computed tomography could not, however, distinguish structures <1 mm in length or determine how the microcrack segments linked to form longer cracks that could transfer larger displacements. Here, the tomographic reconstructions of typical microcrack structures in the 1900-year-old mortar (Fig. 6) provides new insights into fine-scale crack processes and how these may contribute to preserving the integrity of the concrete over many episodes of fracture.

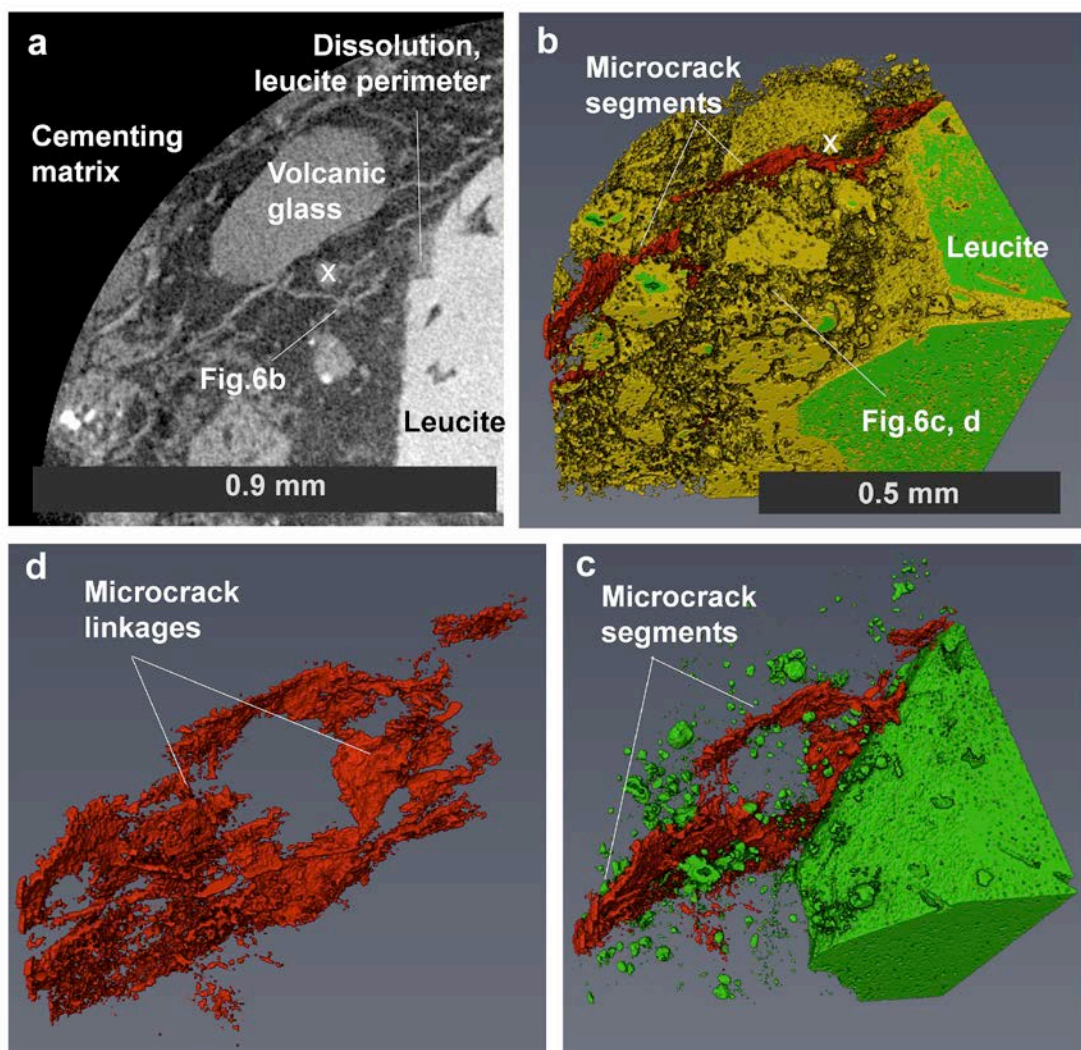


Fig. 6. Reconstruction of typical microcrack segments and linkages. a) 2D tomographic image showing cracks with crystalline fillings, including calcite, in the cementing matrix (dark grey) near a large leucite crystal (light gray) (see also Fig. 4). b) 3D segmentation of mortar components, volcanic aggregate (yellow), cementing matrix (grey), pores (green), and *en echelon* microcrack segments (red). c, d) 3D reconstruction of a segment bridging overlap between two microcrack segments, and finer-scale microcracks with high surface area in the linkage zones.

The 2D tomographic image of the mortar (Fig. 6a) shows microcracks composed of segments mainly <0.3 mm that propagated through the cementitious matrix adjacent to a large leucite crystal. The 3D segmentation (Fig. 6b) illustrates two *en echelon* microcrack segments with a 0.1–0.2 mm



wide offset. A 3D reconstruction nearby (Fig. 6c, d) shows two crack segments with a bridging overlap. The offset between the crack segments is also 0.1–0.2 mm. Linkage was accompanied by a complex zone of microcrack segments  $\leq 100\ \mu\text{m}$ . The reconstruction indicates that the composite crack array has a far higher surface area than could be inferred from a 2D image slice. This indicates that the energy required to propagate and link the microcracks across the *en echelon* offset is quite high. This may result, in part, from obstacles presented by scoria (Fig. 6a, b, location x). Furthermore, pervasive reinforcement of the C-A-S-H binder with strätlingite plates (Figs. 1, 2) could possibly have presented additional obstacles to microcrack propagation at the micrometre scale.

Petrographic images of the Great Hall mortar show the *en echelon* tips of two microcrack segments and the rupture of two scoria clasts by the left segment (Fig. 7). The overlapping microcrack segments are similar to those in the 3D reconstruction (Fig. 6 c, d), except that the crack tips propagated away instead of towards each other. Calcite crystals grew in the open space between the crack walls of both segments. The calcite could potentially seal some crack surfaces and, possibly, create obstacles to further microcrack propagation over time. Autogenous alteration of vaterite and long-term carbonation of C-A-S-H binder could have produced the calcite textures.

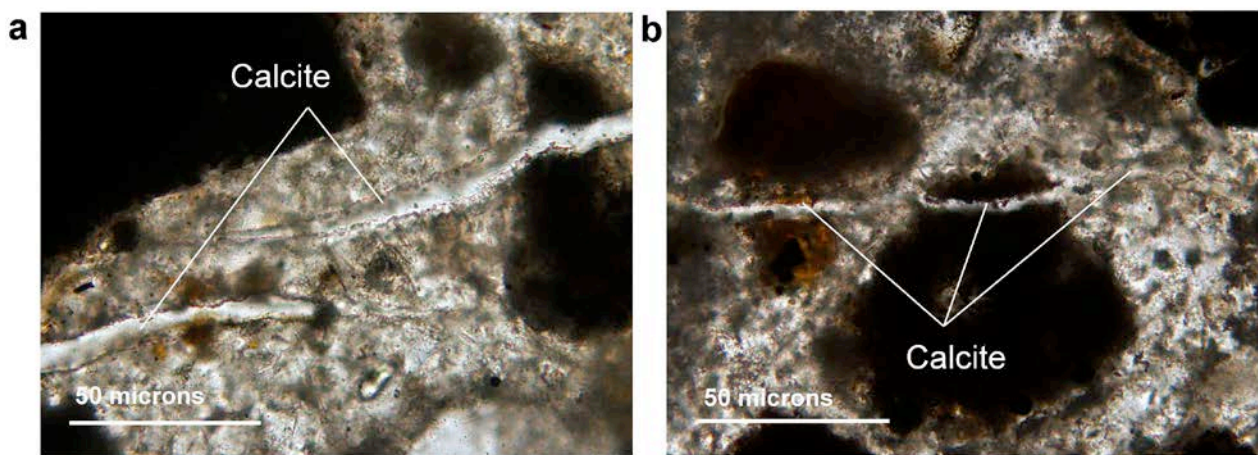


Fig. 7. Petrographic images, plane polarized light, in the Great Hall mortar. a) *en echelon* overlap between two microcrack segments. b) rupture of microscoria by the left segment. Calcite crystals form selvages along the crack walls or nearly entirely fill the void space.

## Summary

Microstructural investigations integrating petrographic microscopy, X-ray microdiffraction analyses and X-ray microtomography studies indicate that the influence of sub-millimetre scale porosity on the durability conglomeratic wall concrete at the Markets of Trajan, Rome, is mitigated by autogenous crystallization of cementitious minerals. The micro-scale porosity is composed mainly of vesicles in sand- and gravel-sized scoria aggregate, sub-spherical pores, up to 2 mm in diameter, and segmented microcracks, up to several mm in length. Petrographic microscopy and X-ray microdiffraction analyses reveal that crystals of strätlingite, a resilient, layered calcium-aluminium-silicate mineral, occur in scoria vesicles, the interfacial zones of scoria aggregate with the cementing matrix, and the cementing matrix itself. In addition, complex intergrowths of crystals ranging from 10–200  $\mu\text{m}$  in length traverse sub-spherical pores. 3D tomographic reconstruction of one such pore indicates that the crystal plates have diverse orientations, and the potential to block propagation of microcracks across relict void space.

Microcracks occur in the mortar as segmented structures, usually  $\leq 0.3\ \text{mm}$ , frequently with *en echelon* offsets. 3D tomographic reconstruction of a linkage across a bridging offset between two microcrack segments reveals a complex zone of fine-scale microcracks. The high crack surface area shown by the reconstruction indicates that propagation and linkage of microcrack segments to produce longer cracks that carry larger displacements requires high fracture energy. Sand- and

gravel-sized scoria present obstacles to crack propagation, causing segment offsets that increase overall toughness. In fracture testing experiments of a reproduction of the Trajanic wall mortar, fine strätlingite crystals  $\leq 5 \mu\text{m}$  in length presented obstacles to microcrack propagation. The larger strätlingite plates in the 1900-year-old mortar may have a similar, or heightened, influence on increasing fracture toughness in the concrete walls. The microcracks themselves may contribute only minimally to increased porosity in the host mortar. This is because calcite selvages or fillings occupy many crack segments.

The large size of strätlingite crystals and their complex intergrowths in diverse components of the ancient mortar suggest long-term crystallization processes involving highly potassic scoriaceous volcanic ash. Introduction of moisture into the concrete structures could have encouraged alkali-activated, post-pozzolanic strätlingite growth in pores and interfacial zones of the hardened concrete. Strätlingite crystals have a relatively low bulk modulus of 23(2) GPa [16] due, in part, to their layered structure. Even so, they may reinforce the cementing matrix in the same way that polypropylene microfibers reinforce Portland cement concrete [17] and contribute to higher fracture toughness. Calcite crystallization that binds the walls of the microcracks contributes to self-healing in the concrete and, perhaps, increased fracture toughness as well. Long-term autogenous reactions in the volcanic ash mortar produced mineral textures in micropores and microcracks that greatly enhanced the mechanical resilience of the ancient concrete.

## Acknowledgment

We thank Massimo Vitti and Lucrezia Ungaro at the Sovrintendenza Capitolina Beni Culturali di Roma Capitale, Ufficio Fori Imperiali, Rome for collaborative research support over many years. T. Teague and Hans-Rudolf Wenk also provided research support. Martin Kunz, Nobumichi Tamura, and Cagla Meral assisted with data acquisition at beamline 12.3.2, Advanced Light Source, Lawrence Berkeley Laboratories, supported by the Director of the Office of Science, Department of Energy, under Contract DEAC02-05CH11231. This research was partly supported by the Singapore Ministry of Education Academic Research Fund Tier 1.

## References

- [1] L. Ungaro, *Il Museo dei Fori Imperiali nei Mercati di Traiano*, Milano 2007.
- [2] L.M. Ungaro, M.; Vitti, M., *Il sistema museale dei Fori Imperiali*, *Simulacra Romae*, Biblioteca Virtuale Cervantes, Alicante, (2013) 12-38.
- [3] A. Frepoli, F. Marra, C. Maggi, A. Marchetti, A. Nardi, N. Pagliuca, M. Pirro, Seismicity, seismogenic structures, and crustal stress fields in the greater Rome area (central Italy), *Journal of Geophysical Research: Solid Earth*, 115 (2010).
- [4] P.A. Galli, D. Molin, Beyond the damage threshold: the historic earthquakes of Rome, *Bulletin of Earthquake Engineering*, 12 (2014) 1277-1306.
- [5] P. Brune, R. Perucchio, Roman concrete vaulting in the Great Hall of Trajan's Markets: Structural evaluation, *Journal of Architectural Engineering*, 18 (2012) 332-340.
- [6] M.D. Jackson, J.M. Logan, B.E. Scheetz, D.M. Deocampo, C.G. Cawood, F. Marra, M. Vitti, L. Ungaro, Assessment of material characteristics of ancient concretes, *Grande Aula, Markets of Trajan, Rome*, *Journal of Archaeological Science*, 36 (2009) 2481-2492.
- [7] J. Ding, Y. Fu, J. Beaudoin, Strätlingite formation in high-alumina cement—zeolite systems, *Advances in Cement Research*, 7 (1995) 171-178.
- [8] M. Jackson, D. Deocampo, F. Marra, B. Scheetz, Mid - Pleistocene pozzolanic volcanic ash in ancient Roman concretes, *Geoarchaeology*, 25 (2010) 36-74.
- [9] P. Brune, A. Ingraffea, M. Jackson, R. Perucchio, The fracture toughness of an Imperial Roman mortar, *Engineering Fracture Mechanics*, 102 (2013) 65-76.
- [10] M.D. Jackson, E.N. Landis, P.F. Brune, M. Vitti, H. Chen, Q. Li, M. Kunz, H.-R. Wenk, P.J. Monteiro, A.R. Ingraffea, Mechanical resilience and cementitious processes in Imperial Roman architectural mortar, *Proceedings of the National Academy of Sciences*, 111 (2014) 18484-18489.

- [11] A. Hillerborg, Results of three comparative test series for determining the fracture energy  $G_F$  of concrete, *Materials and Structures*, 18 (1985) 407-413.
- [12] F. Massazza, Pozzolana and pozzolanic cements, *Lea's chemistry of cement and concrete*, 4 (1998).
- [13] G.S. Aldrete, *Floods of the Tiber in ancient Rome*, JHU Press 2007.
- [14] M. Jackson, F. Marra, R. Hay, C. Cawood, E. Winkler, The judicious selection and preservation of tuff and travertine building stone in ancient Rome, *Archaeometry*, 47 (2005) 485-510.
- [15] R. Rinaldi, M. Sacerdoti, E. Passaglia, Strätlingite: crystal structure, chemistry, and a reexamination of its polytype vertumnite, *European Journal of Mineralogy*, (1990) 841-850.
- [16] J.-h. Moon, J.E. Oh, M. Balonis, F.P. Glasser, S.M. Clark, P.J. Monteiro, Pressure induced reactions amongst calcium aluminate hydrate phases, *Cement and Concrete Research*, 41 (2011) 571-578.
- [17] C. Ostertag, C. Yi, Crack/fiber interaction and crack growth resistance behavior in microfiber reinforced mortar specimens, *Materials and structures*, 40 (2007) 679-691.